

**This is the accepted manuscript version of the contribution published as:**

Wu, M.M., Liang, Y., **Taubert, F., Huth, A.**, Zhang, M., Wang, X. (2023):  
Sensitivity of forest composition and productivity to climate change in mixed broadleaved-Korean pine forest of Northeastern China  
*Ecol. Model.* **483** , art. 110434

**The publisher's version is available at:**

<https://doi.org/10.1016/j.ecolmodel.2023.110434>

1 **Sensitivity of forest composition and productivity to climate change in**  
2 **mixed broadleaved-Korean pine forest of Northeastern China**

3

4 Mia M. Wu<sup>1</sup>, Yu Liang<sup>1,2</sup>, Franziska Taubert<sup>3,4</sup>, Andreas Huth<sup>3,4,5</sup>, Min Zhang<sup>1</sup>, Xugao  
5 Wang<sup>1,2</sup>

6 1. CAS Key Laboratory of Forest Ecology and Management, Institute of Applied  
7 Ecology, Chinese Academy of Sciences, Shenyang 110016, China

8 2. Key Laboratory of Terrestrial Ecosystem Carbon Neutrality, Liaoning Province,  
9 Shenyang 110016, China

10 3. Department of Ecological Modelling, Helmholtz Centre for Environmental  
11 Research – UFZ, 04318 Leipzig, Germany

12 4. German Centre for Integrative Biodiversity Research (iDiv), Halle-Jena-Leipzig,  
13 04103 Leipzig, Germany

14 5. Institute of Environmental Systems Research, University of Osnabrück, 49076  
15 Osnabrück, Germany

16 Correspondence: wangxg@iae.ac.cn (X. Wang)

17 **Abstract**

18 Temperate forest is one of the largest forest biomes and is undergoing remarkable shifts  
19 in forest composition and ecosystem productivity under warming climates. However,  
20 there are considerable uncertainties when predicting future dynamics of temperate  
21 forest ecosystems partly because of the uncertainties in future climate predictions.  
22 Sensitivity analysis provides an effective mean to evaluate the uncertainties in the  
23 predicted forest responses to climate change. Here we evaluated the sensitivity of forest  
24 composition and productivity to climate change in the mixed broadleaved-Korean pine  
25 forest, a keystone temperate forest type in northeast China. In this study, we used a  
26 process-based forest dynamic model, FORMIND, to simulate and predict the response  
27 of the mixed broadleaved-Korean pine forest under climate change based on plant  
28 functional types (PFTs), and we performed model calibration using forest investigation.  
29 We then designed a factorial experiment to quantify the sensitivity to temperature and  
30 precipitation of forest composition and ecosystem productivity. Results showed that the  
31 uncertainty in future climate predictions could result in divergent responses of forest  
32 composition and ecosystem productivity to climate change over the 21st century. The  
33 response of PFTs to climate (temperature and precipitation) varied in terms of  
34 aboveground biomass. Both shade-tolerant and shade-intolerant PFTs exhibited higher  
35 sensitivity ( $> 80\%$  for most of the PFTs) to temperature than precipitation, yet they  
36 responded oppositely to climate warming with shade-tolerant PFTs generally increasing  
37 but shade-intolerant PFTs decreasing. Moderate shade-tolerant PFTs showed higher  
38 precipitation sensitiveness ( $> 50\%$ ). Such differences in response and sensitivity of  
39 PFTs to climate change are related to PFTs' competitiveness. Ecosystem productivity  
40 exhibited a higher sensitivity ( $\geq 50\%$ ) to temperature than to precipitation. There was  
41 more increase in ecosystem respiration than gross primary productivity (GPP) under  
42 warming climate, leading to a decrease in carbon sequestration and net ecosystem  
43 exchange (NEE). Our study addresses the importance of evaluating the sensitivity of a  
44 forest ecosystem model to climate change, which is relatively less studied. The insight

45 from the study may help design effective forest management strategies to cope with  
46 future climate change.

47

48 **Keywords:** climate sensitivity; aboveground biomass; net ecosystem exchange;  
49 FORMIND model

50

## 51 **1. Introduction**

52 Temperate forest is an important component of terrestrial ecosystems. With carbon  
53 reservoirs up to over 50 Pg C (Thurner et al. 2014), these forests play an important role  
54 in regulating the global carbon cycle and mitigating climate change (Bonan 2008; Piao  
55 et al. 2009). Temperate forests are sensitive to changing climates and have been  
56 undergoing remarkable and significant shifts in forest composition (Taylor et al. 2017;  
57 Thom et al. 2017). Consequently, ecosystem productivity associated with the  
58 composition change along with tree growth, carbon consumption, and tree respiration,  
59 is also expected to change (Boisvenue and Running 2006; Brzostek et al. 2014). The  
60 fifth assessment report of the Intergovernmental Panel on Climate Change (IPCC5)  
61 predicted that annual average temperature will increase by 0.5-8.9 °C and precipitation  
62 will increase by 2.5-76.2%, in the middle and high latitudes of northern hemisphere in  
63 the 21<sup>st</sup> century (IPCC 2013). The potential forest responses to climate change may be  
64 considerably varied across a broad range of climate projections (Ahlström et al. 2012;  
65 Huang et al. 2021). Accurate evaluation of temperate forest responses to future climate  
66 change is of great importance with respect to coping with global changes, designing  
67 adaptable forest management strategies, and maintaining its biodiversity.

68 The mixed broadleaved-Korean pine (*Pinus koraiensis* Sieb. et Zucc.) forest is  
69 most significant among temperate forest ecosystems in northeast China because of its  
70 broad distribution and rich species diversity (Krestov et al. 2015). Research suggests  
71 that species composition of mixed broadleaf-Korean pine forest could shift from pine-  
72 to broadleaf-dominated under warming climates (He et al. 2005; Lyu et al. 2017; Shao  
73 et al. 2003; Zhang et al. 2014). For example, many studies report that warming could

74 potentially favor broadleaf species, such as *Quercus* and *Acer* (He et al. 2005; Kim et  
75 al. 2020). The enhanced competitive capacity of the broadleaf species could promote  
76 their growth and colonization, leading to an increase in their proportion and biomass in  
77 the forests (He et al. 2005; Shao et al. 2003). Meanwhile, dendrochronological studies  
78 show that temperature is a predominant factor affecting the growth of Korean pine (Lyu  
79 et al. 2017; Wang et al. 2019). Elevated temperature along with the prolonged growing  
80 season can benefit the establishment of Korean pine and cause an expansion of their  
81 leading edge (Li et al. 2011). Furthermore, studies found a synergistic effect of heat and  
82 moisture on the growth of Korean pine (Zhuang et al. 2017). Particularly, increased  
83 precipitation can strengthen the positive effects of warming on Korean pine, while  
84 decreased precipitation can weaken the growth due to drought stress (Cao et al. 2019;  
85 Wang et al. 2019; Zhuang et al. 2017). Thus, the discrepancies in the responses of mixed  
86 broadleaf-Korean pine forest to climate change may obscure our understanding of the  
87 response of the forest ecosystem to climate change.

88 The mixed broadleaved-Korean pine forest is also expected to significantly change  
89 its ecosystem productivity under warming climate (Qiu et al. 2014; Wang et al. 2019;  
90 Zhou et al. 2011). However, the direction of this change is uncertain. Generally, it is  
91 thought that relatively low temperature is a major constraint to tree growth in this forest  
92 (Cao et al. 2019). Warming should therefore increase the period of photosynthesis by  
93 prolonging the growing season, leading to increases in tree growth, forest biomass, and  
94 productivity, and further promoting carbon sequestration in the ecosystem (Cao et al.  
95 2019; Cao et al. 2018; Zhou et al. 2011). Yet, other studies report that higher  
96 temperatures, especially when accompanied by an asynchronous increase in  
97 precipitation, may lead to higher evapotranspiration, slower tree growth, decreased  
98 forest biomass and productivity, and lower sequestered carbon (Liang et al. 2016;  
99 Wang et al. 2019). Additionally, elevated temperature could also increase maintenance  
100 respiration, further reducing ecosystem productivity (Wang et al. 2019). Increased  
101 drought events under higher temperatures could also result in a shift from carbon sink  
102 to carbon source in the mixed broadleaved-Korean pine forest (Lee et al. 2021; Peng et

103 al. 2009).

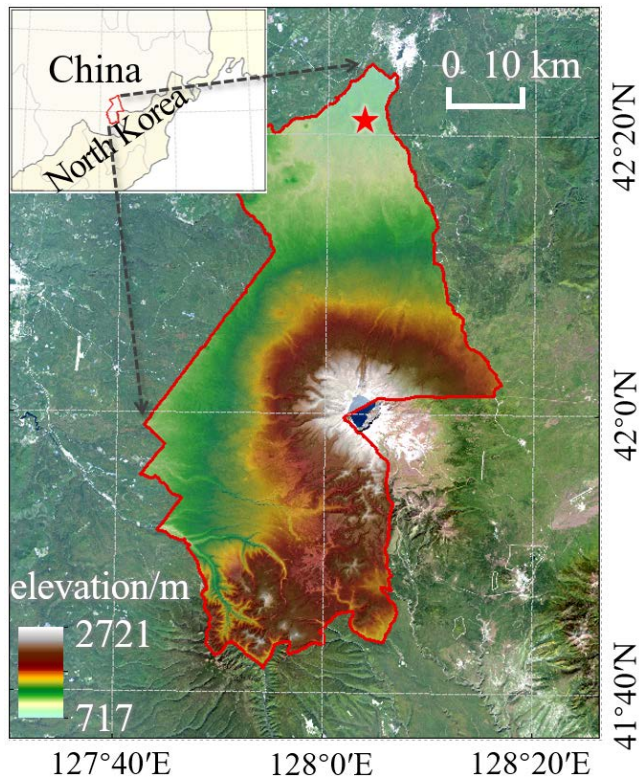
104 In this study, we investigate the response of the mixed broadleaf-Korean pine forest  
105 of Northeast China to climate warming. We used the process-based forest growth model  
106 FORMIND to simulate forest dynamics under various climate scenarios. The model  
107 simulates tree growth and forest development, as well as carbon dynamics, dependent  
108 on climatic conditions. Thus, FORMIND could evaluate the sensitivity of forest  
109 ecosystems to climate change. Sensitivity analysis provides an effective mean to  
110 evaluate the uncertainties in forest responses to climate warming (Huang et al. 2021).  
111 It can also quantify how variations of climate variable such as temperature and  
112 precipitation affect the projected results. The objectives of this study are to (1) develop  
113 a FORMIND modeling framework for the mixed broadleaved-Korean pine forest, (2)  
114 examine the forest dynamics in response to future climates, and (3) quantify the  
115 sensitivity of forest composition and productivity to potential changes in temperature  
116 and precipitation in the mixed broadleaved-Korean pine forest of northeastern China.

117

## 118 **2. Methods and materials**

### 119 2.1 Study site

120 The study focuses on the temperate forests of the Changbai Mountain, northeast  
121 China, bordering North Korea (Fig. 1). Our study site (42°23'N, 128°05'E) is located  
122 in the old-growth mixed broadleaf-Korean pine forest. The mixed broadleaf-Korean  
123 pine forest is a typical temperate forest type of China. The elevation is about 800 m  
124 a.s.l. Climate is a moist temperate climate with long, cold winter and short, warm  
125 summer. The average temperature is 2.8 °C, and the average annual precipitation is  
126 about 700 mm with a wet season from June to September. There are a variety of tree  
127 species, and six dominant species of which represent 90% of total basal area, including  
128 *Pinus koraiensis* Siebold & Zucc., *Tilia amurensis* Rupr., *Acer mono* Maxim., *Quercus*  
129 *mongolica* Fisch. ex Ledeb., *Fraxinus mandschurica* Rupr., and *Ulmus davidiana*  
130 Planch. var. *japonica* (Rehd.) Nakai.



131

132 Figure 1. The location of study site. The red line and the red star indicate Changbai  
 133 Mountains Nature Reserve (CMNR) and study site, respectively.

134

2.2 Inventory data

135

In 2004 a 25-ha (500 m × 500 m) permanent plot was established in our study site,  
 136 which is located within the Changbai Mountain Nature Reserve (CMNR) (Hao et al.  
 137 2008). The plot consists of a multi-layered uneven-aged forest with a dominant tree  
 138 layer of approximately 300 years and an average height of about 26 m. The plot has an  
 139 average elevation of 801.5 m, ranging from 791.8 m to 809.5 m asl. The terrain of the  
 140 plot is generally flat with the exception of some undulating areas. Since the  
 141 establishment of permanent plot, all trees in the plot were censused in five-year  
 142 intervals. For each tree with a diameter at breast height (DBH) ≥ 1 cm, the coordinates,  
 143 species names, DBH, tree height, and crown width were measured and recorded. Thus,  
 144 average basal area and tree density in the plot can be derived. The successive tree census  
 145 also allowed us to capture tree regeneration, growth, and mortality.

146

147

2.3 Climate data

148 To assess the sensitivity of forest to climate change, we collected current and future  
 149 climate data in our study site. The current weather data is derived from the  
 150 meteorological station within the study site, which collects hourly temperature,  
 151 precipitation, solar radiation, wind speed, and relative humidity from 2004-2019.  
 152 Future climate (temperature and precipitation) data (2015-2100) is derived from CMIP6  
 153 global climate models (GCMs) over the 21<sup>st</sup> century ([https://esgf-  
 154 node.llnl.gov/projects/cmip6/](https://esgf-node.llnl.gov/projects/cmip6/)), which are based on simulations of the Earth's climate  
 155 system. Future climate predictions (2015-2100) of this region largely indicated that  
 156 both temperature and precipitation will exhibit increasing trends, but at different  
 157 magnitudes. Thus, we chose four typical climatic scenarios (CESM2-WACCM SSP245,  
 158 CESM2-WACCM SSP370, CNRM-ESM2 SSP245, and CNRM-ESM2 SSP585),  
 159 representing warmer and wetter, much warmer and wetter, warmer and much wetter,  
 160 and much warmer and much wetter climate at the end of 21<sup>st</sup> century (2080-2100),  
 161 respectively, relative to current condition, which can capture the potential future climate  
 162 change characteristics (Table 1, Fig. S1). Moreover, the chosen future climate scenarios  
 163 whose predictions in 2015 are closest to the weather data of the meteorological station.  
 164 All selected climate scenarios have inherited daily climate variability and consequently  
 165 annual variability similar to the current climate data (e.g., greatest precipitation occurs  
 166 in the summer and snow in the winter). Specifically, we used the PRISM (parameter-  
 167 elevation regressions on independent slopes model) interpolation method (Daly et al.  
 168 2002) that included elevation of Changbai Mountain to spatially interpolate the future  
 169 climate data for our study site.

170

171 Table 1. The characteristics of current climate and future climate scenarios at the end  
 172 of 21<sup>st</sup> century.

<b>climate scenario</b>	<b>average T (°C)</b>	<b>average annual P (mm)</b>	<b>ΔT (°C)</b>	<b>Δ annual P (mm)</b>	<b>climate characteristic</b>
current	3.7	705.1	-	-	-



---

(2005-2015)						
CESM2-WACCM						
SSP245	7.1	1162.5	3.4	457.4		warmer and wetter
(2080-2100)						
CESM2-WACCM						
SSP370	9.1	1155.9	5.4	450.8		much warmer and wetter
(2080-2100)						
CNRM-ESM2						
SSP245	6.3	1278.0	2.6	572.9		warmer and much wetter
(2080-2100)						
CNRM-ESM2						
SSP585	9.3	1290.5	5.6	585.4		much warmer and much wetter
(2080-2100)						

---

173 Note:  $\Delta T$  and  $\Delta$ annual P represent the changes in annual mean temperature and annual  
174 precipitation between current (2004-2019) and future climate conditions at the end of  
175 21<sup>st</sup> century (2080–2100), respectively.

176

#### 177 2.4 FORMIND Model

178 The FORMIND model is a process-based, individual-oriented, spatially explicit  
179 forest model, which was designed for simulating the dynamics of species-rich forest  
180 communities. It divides the simulated forest area into patches (20 m × 20 m) interacting  
181 by seed dispersal and tree falling. Within each patch, FORMIND simulates tree  
182 demographic processes, including tree growth, recruitment, competition, and mortality,  
183 which are mainly controlled by the availability of light and space. Tree biomass growth  
184 is determined with respect to a carbon balance as a result of photosynthesis and  
185 respiration, which regulates the increments in tree height, stem diameter, stem volume,  
186 and leaf area. In FORMIND, seeds are stochastically distributed among the patches,  
187 and new seedlings can establish under suitable light conditions (Fischer et al. 2016).  
188 Both seed survival and establishment can be influenced by climate change, which

189 consequently regulates forest regeneration. Tree competition takes place for light owing  
190 to shading effects, as well as for space owing to expanded canopies. Tree mortality is  
191 associated with weakened tree growth (related to climate), enhanced competition for  
192 space (e.g., self-thinning), death of large trees and their falling, as well as background  
193 mortality due to stochastic events, which can be simulated stochastically. The  
194 FORMIND model does not simulate asexual reproduction (e.g., sprouting, layering)  
195 that many trees are capable of and that is important in more disturbance-prone forest  
196 ecosystems. Since the study location is not generally affected by these perturbations,  
197 this limitation should not have an appreciable impact on our simulations and we have  
198 thus chosen to exclude this regeneration process. More model details are available in  
199 the supplementary materials.

200 The FORMIND model is capable of simulating forest carbon dynamics (Bohn et  
201 al. 2014; Fischer et al. 2016). Based on physiological processes such as photosynthesis  
202 and respiration, it analyzes the local carbon fluxes among atmosphere, vegetation, and  
203 soil to estimate gross primary productivity (GPP), respiration of the forest (including  
204 living biomass and dead biomass) and the soil, and net ecosystem exchange (NEE).  
205 NEE is calculated as the difference between the ecosystem GPP and the total respiration  
206 by the forest and soil. Thus, a positive NEE represents increasing carbon stocks, while  
207 a negative NEE represents decreasing carbon stocks.

208

## 209 2.5 Model parameterization

210 FORMIND simulates forest dynamics based on plant function types (PFTs) which  
211 represents the groups of tree species with similar traits. Here, according to physiological  
212 attributes including maximum potential tree height and light requirement (shade-  
213 tolerance), we classified the species in our area into seven PFTs (Table 2). We  
214 determined the maximum potential tree height classes by referring to the criteria from  
215 Groeneveld et al. (2009), together with the vertical structure (i.e., height layers) of the  
216 forest in the study site. We conducted the parameterization of the FORMIND model by  
217 defining environmental variables as well as model parameters describing tree

218 establishment, mortality, geometry, and biomass production. In this study, we defined  
 219 the allometry relations for tree geometries (e.g., diameter-height relationships) for each  
 220 PFT from the aforementioned permanent plot encompassing a range of sizes and ages  
 221 of trees (Table S2). Specifically, we recorded DBH and height for each individual tree  
 222 every five years (2004-2019). Furthermore, the seed number of each PFT is determined  
 223 from the published results in the study site (Qian et al. 2019). The environmental  
 224 parameters and variables include those related to light condition, soil, and climate. The  
 225 parameters referring to light condition and soil were obtained from related literature  
 226 and field investigation. The climatic parameters were derived from the climate station  
 227 (current climate) and CMIP6 future predicted data (see above) in the study site, such as  
 228 temperature, precipitation. Here, we did not simulate CO<sub>2</sub> concentration since we opted  
 229 to simplify the parameterization. The parameters related to mortality and biomass  
 230 production for each PFT were estimated from multiple successive censuses (2004-2014  
 231 by every five years). In order to better reproduce each PFT's growth dynamic, we also  
 232 inventoried an early successional forest plot (24 ha), whose data were used as references  
 233 point to adjust the diameter growth change parameters. The plot (42°22'N, 128°00'E)  
 234 is dominated by white birch (*Betula platyphylla* Suk.) and aspen (*Populus davidiana*  
 235 Dode), and is located near the study site. Within the plot, the geographic coordinates,  
 236 height, and DBH of all trees (DBH ≥ 1 cm) were recorded. In this study, we performed  
 237 simulations based on PFTs rather than on individual tree species, since parameters at  
 238 the tree species level may introduce uncertainties without gaining more significant  
 239 insights.

240

241 Table 2. Seven plant functional types (PFTs) divided by shade-tolerance and potential  
 242 maximum height class of tree species in the mixed broadleaved-Korean pine forest

<b>PFT</b>	<b>shade- tolerance class*</b>	<b>potential maximum height (H<sub>max</sub>) class**</b>	<b>tree species</b>
S1H2	1	2	<i>Betula platyphylla</i> Suk., <i>Betula costata</i> Trautv., <i>Populus</i>

---

			<i> davidiana</i> Dode, <i>Syringa reticulata</i> subsp. <i>amurensis</i> (Ruprecht) P. S., <i>Phellodendron amurense</i> Rupr.
S1H3	1	3	<i>Populus ussuriensis</i> Kom., <i>Quercus mongolica</i> Fisch. ex Ledeb.
S2H2	2	2	<i>Maackia amurensis</i> Rupr. et Maxim., <i>Ulmus laciniata</i> (Trautv.) Mayr.
S2H3	2	3	<i>Ulmus davidiana</i> Planch. var. <i>japonica</i> (Rehd.) Nakai, <i>Fraxinus mandshurica</i> Rupr.
S3H1	3	1	<i>Sorbus pohuashanensis</i> (Hance) Hedl., <i>Sorbus alnifolia</i> (Sieb. et Zucc.) K. Koch
S3H2	3	2	<i>Acer mono</i> Maxim., <i>Acer mandshuricum</i> Maxim., <i>Acer triflorum</i> Komarov, <i>Malus baccata</i> (L.) Borkh., <i>Tilia mandshurica</i> Rupr. et Maxim.
S3H3	3	3	<i>Pinus koraiensis</i> Sieb. et Zucc., <i>Tilia amurensis</i> Rupr.

---

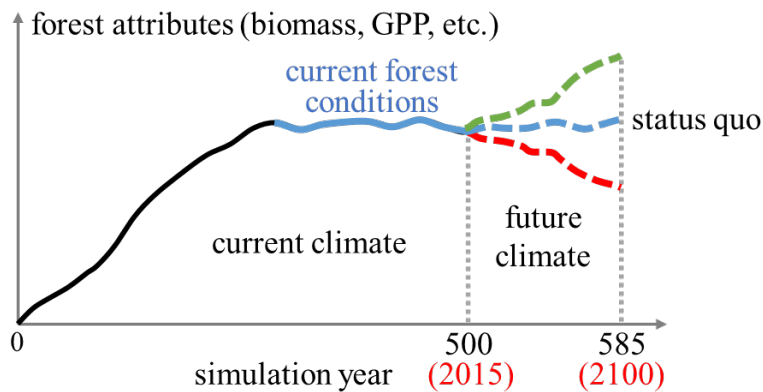
243 Note: \*Shade-tolerance class: 1: least shade-tolerance; 2: middle shade-tolerance; 3:  
244 most shade-tolerance. \*\*Potential maximum height ( $H_{\max}$ ) classes: 1:  $H_{\max} \leq 15$  m; 2:  
245  $15 \text{ m} < H_{\max} \leq 25$  m; 3:  $H_{\max} > 25$  m.

246

## 247 2.6 Model simulation

248 We simulated forest succession on 25 ha over a period of 585 years with a 1-year  
249 time step, initializing with bare ground. During the first 500 years, forest dynamics  
250 were simulated in the stable climatic conditions to allow forest to reach a steady state  
251 (corresponding to the current old-growth forests), which is designed for the model spin-  
252 up to reach equilibrium (Fig. 2). We then ran the model for the next 85 years (which  
253 correspond to years 2015-2100, i.e., CMIP6 projection period) to simulate future forest  
254 dynamics under the predicted climatic scenarios (see “climate data” section) in order to  
255 evaluate the sensitivity of the forest to future climate changes. Generally, under  
256 uncertain future climate changes, forest attributes will exhibit three possible scenarios:  
257 “status quo” (the relatively stable current forest condition) as the null hypothesis, and

258 either higher or lower levels as alternative outcomes (Fig. 2). Additionally, we also  
 259 included a simulation scenario with no future climate change as baseline. In this study,  
 260 we performed the simulation for 10 replications. Not all simulation results will be  
 261 presented in this paper, please see the supplemental materials section for these  
 262 outcomes.



263

264 Figure 2. Schematic diagram of forest stand development initialized from bare land.  
 265 Under future climate, there are three possible scenarios of forest attributes (such as  
 266 biomass, GPP), including “status quo” (the relatively stable current forest condition) as  
 267 the null hypothesis, and either higher or lower levels as alternative outcomes.

268

## 269 2.7 Model calibration

270 For model calibration, we compared the simulated mature forests with the  
 271 corresponding field observations. Based on the assumption that forests can reach the  
 272 equilibrium state in the late-successional stage under the stable climate conditions  
 273 (Bormann and Likens 1979; Turner et al. 1993), we regarded that the simulated forest  
 274 reached maturity and stabilized after 300 simulation years. Thus, the simulated mature  
 275 forest attributes were averaged over the 300-500 years. Field observation values were  
 276 the averages from 2004-2014 surveys in the study site (25 ha). We conducted model  
 277 calibration by iteratively adjusting the model parameters that cannot be directly  
 278 determined, such as light response curves and minimum light intensity required for seed  
 279 ingrowth (Table S2) until we were able verify that there was no significant difference  
 280 between the simulated results and the field observations (25 ha, mentioned above) in

281 terms of tree density and basal area for each PFTs for all trees. Here, the measured and  
282 estimated basal area for each PFT can be calculated from the average of the basal area  
283 of all trees for each PFT. Model calibration also involved comparing the simulated  
284 results at the early-successional stage against forest inventory data (an early-  
285 successional forest plot near the mixed broadleaved-Korean pine forest plot) (see  
286 Supplementary, Fig. S3). The two-step calibration processes ensured that calibrated  
287 model is capable of reproducing the current mixed forest conditions.

288

## 289 2.8 Climate sensitivity

290 We quantified the sensitivity of forest dynamics in response to future climate  
291 change by the four CMIP6 scenarios (section “climate data”). These scenarios can lead  
292 to a factorial experiment for two independent climate variables at two levels:  
293 temperature (warm and warmer at the end of 21<sup>st</sup> century) and precipitation (wet and  
294 wetter at the end of 21<sup>st</sup> century). For the future scenarios, we used daily values of  
295 temperature and precipitation of the corresponding CMIP6 climate scenarios during  
296 2015-2100. We analyzed final states in the simulated forest under the CMIP6 future  
297 climate scenarios by the averaged values over the last 20 years (2080-2100) to evaluate  
298 the sensitivity of the forest to future climate change.

299

## 300 2.9 Data analysis

301 For all climate scenarios, we assessed the forest composition through the  
302 aboveground biomass (AGB) of each PFT, and ecosystem productivity through gross  
303 primary productivity (GPP), net productivity (NPP), total respiration (R<sub>t</sub>), autotrophic  
304 respiration (R<sub>a</sub>), heterotrophic respiration (R<sub>h</sub>), and net ecosystem exchange (NEE).  
305 Moreover, we regarded the above variables as the response variables when quantifying  
306 the sensitivity of forest composition and productivity in response to climate change for  
307 the end of 21<sup>st</sup> century (2080-2100). We quantified the sensitivity of the response  
308 variables to climate change through determining relative importance of each climatic  
309 variable, by calculating the proportion of the total variance in the response variables

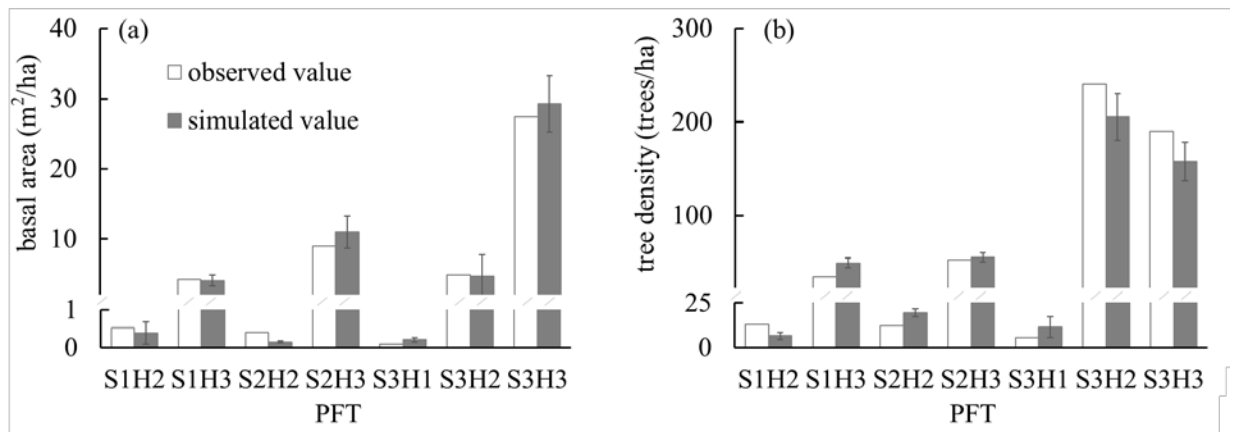
310 explained by each climatic variable using two-way ANOVA (Analysis of Variance)  
 311 based on Type III sums of squares.

312

### 313 3 Results

#### 314 3.1 Model validation

315 Current field inventory data and simulated data exhibited no significant differences  
 316 in either total basal area or density by each PFT (paired t-tests,  $df = 6$ ,  $p < 0.05$ ) (Fig.  
 317 3). This showed that the simulated forest composition and structure using the  
 318 FORMIND model are representative of our field-based example of the mixed  
 319 broadleaved-Korean pine forest.



320

321 Figure 3. Comparison between simulated basal area (a) and tree density (b) in 2015 and  
 322 observed data in 2010s for each PFT.

323

324 The simulated forest development pathways of all PFTs showed that shade-  
 325 intolerant PFTs (S1H2 and S1H3) initially sharply increased but then decreased in AGB,  
 326 and finally get gradually replaced by mid-tolerant and tolerant PFTs (e.g., S2H3, S3H2,  
 327 and S3H3), which exhibited gradual increases and stabilized after 300 years of the  
 328 simulation (Fig. S4). The PFTs with both relative shade tolerance and a higher potential  
 329 maximum height (S3H3, S3H2, and S2H3), became dominant at the steady state (more  
 330 than 90% of total AGB) (Fig. S4). Thus, simulated forest trajectories using the  
 331 FORMIND model were consistent with forest stand development theory (Oliver and  
 332 Larson 1996), which increased our confidence in the ability of the calibrated

333 FORMIND model to effectively represent long-term forest dynamics for the study site.

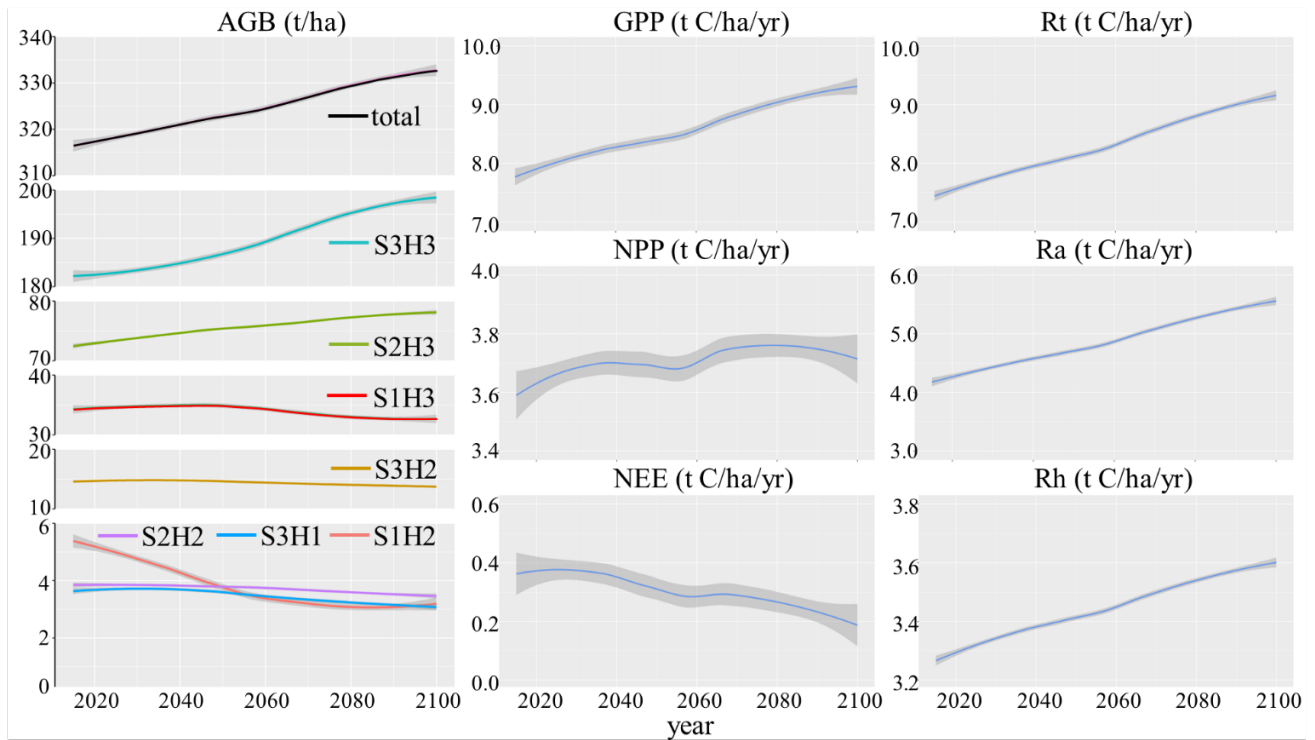
334

### 335 3.2 Forest dynamics under future climates

336 Generally, total AGB showed patterns of gradual increase under all future climate  
337 scenarios, from 317.0 t/ha to  $331.4 \pm 3.0$  t/ha from 2015 to 2100 (Fig. 4). The largest  
338 increase in total AGB occurred in the CNRM-WACCM SSP245 scenario (warmer and  
339 wetter), and the smallest increase occurred in CESM2-ESM2 SSP245 scenario (warmer  
340 and much wetter) (Fig. S5). Notably, the seven PFTs have divergent responses in their  
341 AGB to future climate change. Specifically, for some of the PFTs, including S3H3 and  
342 S2H3, AGB gradually increased over the 21<sup>st</sup> century under future climates, with an  
343 increase of  $15.2 \pm 4.2$  t/ha ( $182.2 - 197.4 \pm 4.2$  t/ha during 2015-2100) and  $5.3 \pm 0.6$  t/ha  
344 ( $72.7 - 78.0 \pm 0.6$  t/ha during 2015-2100) by 2100, respectively. Shade-intolerant PFTs  
345 (S1H2, S1H3), exhibited decreases in AGB with  $1.9 \pm 0.4$  t/ha ( $5.3 - 3.4 \pm 0.4$  t/ha) and  
346  $2.4 \pm 1.3$  t/ha ( $34.8 - 32.4 \pm 1.3$  t/ha) from 2015 to 2100. Other PFTs, like S3H2, S2H2,  
347 and S3H1, kept relatively stable during the years 2015-2100 (Fig. 4).

348 The increases in temperature and precipitation also resulted in noticeable changes  
349 in ecosystem productivity over the 21<sup>st</sup> century. NEE showed an overall slight decline  
350 from 0.3 t C/ha/yr in 2015 to  $0.3 \pm 0.1$  t C/ha/yr in 2100, respectively (Fig. 4). The largest  
351 decrease occurred in CNRM-ESM2 SSP585 scenario (much warmer and much wetter)  
352 with 0.2 t C/ha/yr, while the smallest decrease occurred in CNRM-ESM2 SSP245  
353 scenario (warmer and much wetter), with 0.0 t C/ha/yr (Fig. S6). NPP showed slight  
354 increase under the four future climate scenarios, with 3.6 t C/ha/yr in 2015 to  $3.9 \pm 0.2$  t  
355 C/ha/yr in 2100. The largest NPP occurred in CNRM-ESM2 SSP245 scenario (warmer  
356 and much wetter) (3.8 t C/ha/yr), while the smallest NPP occurred in CESM2-WACCM  
357 SSP245 scenario (warmer and wetter) (3.7 t C/ha/yr) (Fig. S6). Additionally, under the  
358 four climate change scenarios, GPP and respiration (Rt, Ra, and Rh) presented slow  
359 increases of  $1.7 \pm 0.6$  (GPP),  $1.8 \pm 0.6$  (Rt),  $1.4 \pm 0.5$  (Ra), and  $0.4 \pm 0.1$  (Rh) tC/ha/yr,  
360 respectively, during 2015-2100 (Fig. 4). The largest increase occurred in CNRM-ESM2  
361 SSP585 scenario (much warmer and much wetter), while the smallest increase in





363

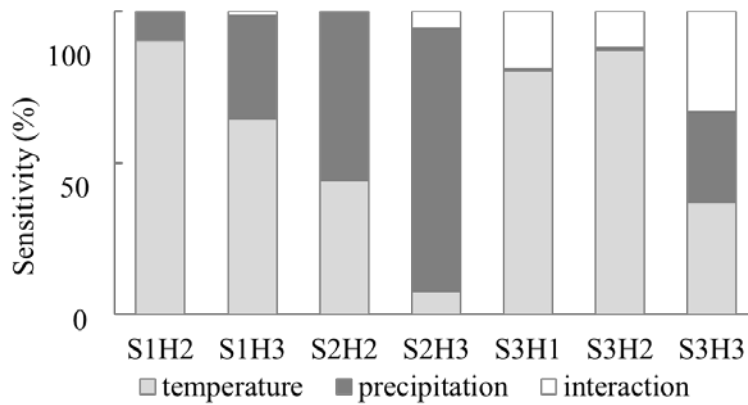
364 Figure 4. The dynamics of average of aboveground biomass (AGB) of individual PFTs,  
 365 total AGB, NEE, GPP, NPP, Rt (total respiration), Ra (autotrophic respiration), and Rh  
 366 (heterotrophic respiration) during the simulated years 2015-2100 across all climate  
 367 scenarios. Grey shading represents the 5%–95% confidence interval (mean  $\pm$  2se  
 368 (standard error)).

369

### 370 3.3 Sensitivity of individual PFTs to climate

371 The sensitivity of seven PFTs to climate (temperature and precipitation) varied.  
 372 Compared to precipitation, most of the PFTs were more sensitive to temperature in  
 373 terms of AGB, including S1H2, S1H3, S3H1, S3H2, and S3H3. Especially, for S1H2,  
 374 S3H1, and S3H2, temperature explained  $>80\%$  of total variation in AGB (Fig. 5). For  
 375 S1H3 and S3H3, temperature and its interaction with precipitation explained  $>65\%$  of  
 376 total variation in AGB. However, AGB of mid shade-intolerant PFTs (S2H2 and S2H3)  
 377 was more sensitive to precipitation than temperature, with precipitation explaining 56.0%  
 378 and 86.9% of total variation in their AGB, and temperature explaining 44.0 % and 7.6%,

379 respectively (Fig. 5).



380

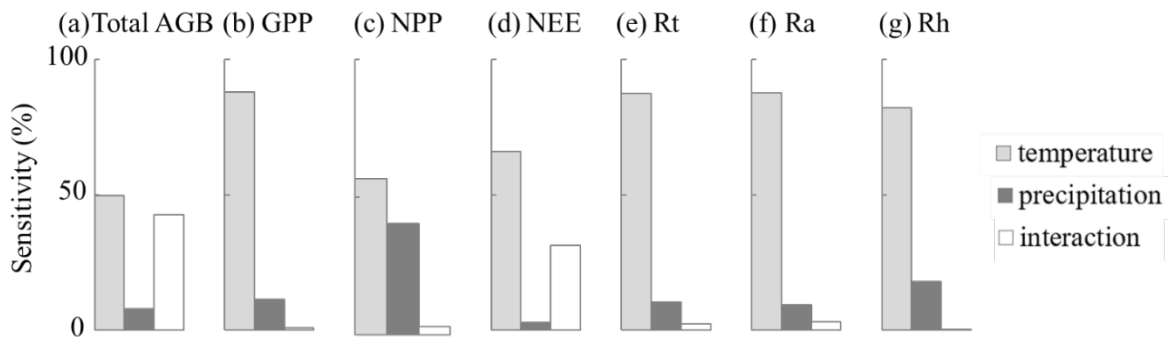
381 Figure 5. The sensitivity of individual PFTs to temperature, precipitation, and their  
 382 interaction in terms of aboveground biomass (AGB).

383

384 3.4 Sensitivity of the forest ecosystem to climate

385 Total AGB exhibited a higher sensitivity to temperature explaining 49.6% of its  
 386 total variation, than to precipitation explaining only 7.7% (Fig. 6a). Meanwhile,  
 387 ecosystem productivity also exhibited a higher sensitivity to temperature than  
 388 precipitation. For GPP, NPP, and NEE, temperature explained 87.8%, 56.7%, and 66.1%  
 389 of their total variation, respectively, exceeding that explained by precipitation (11.4%,  
 390 40.5%, and 2.7%) (Fig. 6b-d). Likewise, respiration (Rt, Ra, and Rh) was also more  
 391 sensitive to temperature than precipitation, with >80% of total variation explained by  
 392 temperature (Fig. 6e-g).

393



394

395 Figure 6. The sensitivity of total aboveground biomass (AGB), GPP, NPP, NEE, Rt, Ra,  
 396 and Rh to temperature, precipitation, and their interaction.

397

#### 398 **4 Discussion**

399 This study is one of the few attempts to apply dynamic forest models, here  
400 specifically FORMIND, to the mixed broadleaved-Korean pine forest – an important  
401 temperate forest in northeast China. Simulated forest dynamics showed that intolerant  
402 pioneer tree species sharply increased in AGB at early successional stages, afterwards  
403 decreased gradually, and finally were replaced by dominant and climax tree species  
404 (mid shade-tolerant and shade-tolerant tree species). The simulated forest successional  
405 trajectories followed the theories of classic forest stand dynamics (Oliver and Larson  
406 1996), which are consistent with the simulated dynamics of other forest ecosystems  
407 (Fischer et al. 2016; Groeneveld et al. 2009). We focused on the AGB dynamics of  
408 individual PFTs (which can reflect the compositional differences through PFT  
409 dominance) and on ecosystem productivity under four representative future climate  
410 scenarios, and evaluated the sensitivity of this forest ecosystem to climate. We found  
411 that the uncertainty in future climate predictions can lead to inconsistent responses of  
412 forest composition and ecosystem productivity to climate change. The sensitivity of the  
413 forest to temperature and precipitation differed within both – plant function type (PFT)  
414 composition and ecosystem productivity. Our study addresses the importance of  
415 evaluating the sensitivity of forest ecosystems to climate change, which is relatively  
416 less studied. The insight from the study may help designing effective forest  
417 management strategies to cope with future climate change.

418 Our results suggest that the simulated forest composition and structure of the mixed  
419 broadleaved-Korean pine forest by the FORMIND model (starting from bare ground to  
420 year 2015) reflected the currently observed forest conditions. Moreover, the simulated  
421 results, with an NEE of 0.3-0.6 t C/ha/yr in ~2015 (Fig. S6), indicated that currently the  
422 forest is still a carbon sink, which agrees with the observations and other simulations at  
423 this forest site (0.3-1.8 t C/ha/yr) (Guan et al. 2006; Saigusa et al. 2013; Tang et al.  
424 2009; Wang et al. 2006; Xie et al. 2020). Moreover, our simulated result is consistent  
425 with other studies in temperate forest worldwide. For example, a study of estimated

426 NEP (which is generally considered to be close to NEE) from improved individual-  
427 based forest ecosystem model (FORCCHN) showed that NEP in mixed broadleaved-  
428 coniferous forests from 1982 to 2011 were 0.4 t C /ha/yr (Zhao et al. 2019). Forest  
429 observation exhibited that the average NEP for unmanaged temperate and boreal forests  
430 more than 200 years old was  $1.3 \pm 0.6$  t C /ha/yr, indicating a slight net C sink  
431 (Gundersen et al. 2021), which is close to our simulation result. The above results  
432 confirmed that the FORMIND model performs well in simulating the forest dynamics  
433 in the studied mixed broadleaved-Korean pine forest. Overall, we found that both  
434 biomass and productivity of the mixed broadleaved-Korean pine forest will show an  
435 increasing trend under future climate change, which is similar to the predicted results  
436 of other temperate forest in northeastern United States (Wang et al. 2017), further  
437 supporting the promoting effects of climate warming on forest carbon accumulation.

438 Our results revealed that there are divergent responses of the PFTs to temperature  
439 and precipitation over the 21<sup>st</sup> century in the mixed broadleaved-Korean pine forest.  
440 The simulated AGB of PFTs is generally more sensitive to temperature than to  
441 precipitation. This is mainly due to the climate of the study site (Changbai Mountain)  
442 with low temperatures and abundant precipitation (Yang 1981), where tree growth is  
443 more responsive to temperature increases. In our study, we found that the least shade-  
444 tolerant and the most shade-tolerant PFTs exhibited a higher sensitivity to temperature  
445 than precipitation, but they showed opposite responses. The most shade-tolerant PFTs  
446 (e.g., Korean pine, basswood) gradually increased in AGB with warming climates,  
447 while the least shade-tolerant PFTs (such as birch, aspen, oak) gradually decreased.  
448 This discrepancy is related to the tree species' biological traits, which affect the species  
449 establishment and survival (Craine and Dybzinski 2013). A tree's ability to increase its  
450 growth under more favorable climates is also confounded by its competition capability  
451 that varies significantly among species (Ford et al. 2017). In our study area, future  
452 increases in temperature and precipitation would create a more suitable environment  
453 for tree growth. However, the shade-tolerant PFTs with strong competitiveness will  
454 gain advantages over other PFTs and occupy more space. In particular, recent studies

455 based on both, model simulation and tree chronology, also confirmed that shade-  
456 tolerant species, such as Korean pine, was highly temperature sensitive and showed a  
457 positive relationship between radial growth and temperature (Lyu et al. 2017; Wang et  
458 al. 2019). However, because of the diminished available space and enhanced tree  
459 competition resulted from the growth and establishment in shade-tolerant PFTs, AGB  
460 of shade-intolerant PFTs with weak competitiveness suffers, even though these PFTs  
461 are also favored under the warming climates. Noteworthy, moderate shade tolerant  
462 PFTs, such as ash and elm group, exhibited lower sensitivity to temperature than  
463 precipitation, and the simulated dynamics in their AGB remain largely stable with slight  
464 fluctuations. This is because their ecological niches are mostly in the middle between  
465 shade-tolerant and shade-intolerant PFTs, allowing them to be less sensitive to climate  
466 change. Therefore, under anticipated climatic conditions in the future, species  
467 composition in mixed broadleaved-Korean pine forest may tend to evolve towards  
468 increasing in shade-tolerant PFTs but decreasing shade-intolerant PFTs. Notably, this  
469 change in forest composition is mainly caused by climate change rather than succession,  
470 as the current forest, i.e., mature forest dominated by mid- to late-successional species,  
471 has been already in a stable state, i.e., the successional climax under the current climate.  
472 Certainly, drought induced by high temperature may limit the increase in forest biomass  
473 (Allen et al. 2010; Ma et al. 2012).

474 We found that ecosystem productivity exhibited a higher sensitivity to temperature  
475 than precipitation in the mixed broadleaved-Korean pine forest. This is consistent with  
476 recent studies based on carbon flux observation (Yu et al. 2008; Yu et al. 2005), which  
477 shows that the low temperature limits tree growth in this forest ecosystem. Future  
478 warming can prolong the growing season and increase tree photosynthesis, thereby  
479 enhancing forest ecosystem productivity (Keenan et al. 2014; Oberbauer et al. 2007).  
480 Our simulation results also found that GPP will increase under future climate scenarios  
481 over the 21<sup>st</sup> century. Meanwhile, our results also suggest that ecosystem respiration  
482 demonstrated a high sensitivity to temperature, which is consistent with recent studies  
483 (Jiang et al. 2005; Wen et al. 2006; Yu et al. 2005). We found that ecosystem respiration

484 showed a gradual increase under the warming climates. This is resulted from the  
485 elevated temperature that increases plant and soil respiration rates (Atkin and Tjoelker  
486 2003; Davidson and Janssens 2006). Although increasing precipitation may increase  
487 soil water content, promoting plant growth and soil respiration, and thus increasing  
488 ecosystem GPP and respiration (Beer et al. 2010; Chen et al. 2013; Wang et al. 2004),  
489 the intensity of the effect is relatively weak due to abundant precipitation in our study  
490 site. We did not find synchronous response of GPP and respiration to climate change in  
491 this study. Instead, we found that respiration increases more strongly than GPP  
492 (photosynthesis) under the warming climates. This could lead to a reduced carbon  
493 sequestration and decreased NEE, which may even change the forest ecosystem from a  
494 carbon sink to a carbon source under the higher temperature increase scenarios. Thus,  
495 the differences in the response and sensitivity of photosynthesis and respiration to  
496 climate change may alter future ecosystem carbon dynamics.

497 Our study that evaluates and quantifies the sensitivity of forest ecosystems to  
498 climate change is crucial in predicting the evolution of ecosystems under future climate  
499 change. Under future warming and precipitation conditions, our simulated results  
500 showed that the aboveground biomass of the forest increases over the 21st century,  
501 accompanied by increases in abundance of shade-tolerant tree species. This suggests  
502 that forest demand of management for promoting shade tolerant species could be  
503 naturally met under the future climate conditions in our study area. However, there were  
504 some limitations in the model simulation. The FORMIND model we used can only  
505 simulate seed-based tree regeneration without asexual reproduction and disturbance,  
506 which may partly limit the capability of the model when predicting future forest  
507 dynamics. We will further explore and discuss these limitations in future work.

508

## 509 **Acknowledgements**

510 This work was supported by the National Natural Science Foundation of China  
511 (31961133027, 31971486, 32171562), the China Postdoctoral Science Foundation  
512 (2022M713293), and the Natural Science Foundation of Liaoning Province (2023-BS-

513 023).

514

515 **References**

516 Ahlström, A., Schurgers, G., Arneeth, A., & Smith, B. (2012). Robustness and  
517 uncertainty in terrestrial ecosystem carbon response to CMIP5 climate change  
518 projections. *Environmental Research Letters*, 7, 044008

519 Allen, C.D., Macalady, A.K., Chenchouni, H., Bachelet, D., McDowell, N., Vennetier,  
520 M., Kitzberger, T., Rigling, A., Breshears, D.D., Hogg, E.T., Gonzalez, P., Fensham, R.,  
521 Zhang, Z., Castro, J., Demidova, N., Lim, J.-H., Allard, G., Running, S.W., Semerci,  
522 A., & Cobbt, N. (2010). A global overview of drought and heat-induced tree mortality  
523 reveals emerging climate change risks for forests. *Forest Ecology and Management*,  
524 259, 660-684

525 Atkin, O.K., & Tjoelker, M.G. (2003). Thermal acclimation and the dynamic response  
526 of plant respiration to temperature. *Trends in plant science*, 8, 343-351

527 Beer, C., Reichstein, M., Tomelleri, E., Ciais, P., Jung, M., Carvalhais, N., Rödenbeck,  
528 C., Arain, M.A., Baldocchi, D., & Bonan, G.B. (2010). Terrestrial gross carbon dioxide  
529 uptake: global distribution and covariation with climate. *Science*, 329, 834-838

530 Bohn, F.J., Frank, K., & Huth, A. (2014). Of climate and its resulting tree growth:  
531 Simulating the productivity of temperate forests. *Ecological Modelling*, 278, 9-17

532 Boisvenue, C., & Running, S.W. (2006). Impacts of climate change on natural forest  
533 productivity—evidence since the middle of the 20th century. *Glob Chang Biol*, 12, 862-  
534 882

535 Bonan, G.B. (2008). Forests and climate change: forcings, feedbacks, and the climate  
536 benefits of forests. *Science*, 320, 1444-1449

537 Bormann, F.H., & Likens, G.E. (1979). *Pattern and Process in a Forested Ecosystem*.  
538 New York: Springer

539 Brzostek, E.R., Dragoni, D., Schmid, H.P., Rahman, A.F., Sims, D., Wayson, C.A.,  
540 Johnson, D.J., & Phillips, R.P. (2014). Chronic water stress reduces tree growth and the  
541 carbon sink of deciduous hardwood forests. *Glob Chang Biol*, 20, 2531-2539

542 Cao, J., Liu, H., Zhao, B., Li, Z., Drew, D.M., & Zhao, X. (2019). Species-specific and  
543 elevation-differentiated responses of tree growth to rapid warming in a mixed forest  
544 lead to a continuous growth enhancement in semi-humid Northeast Asia. *Forest  
545 Ecology and Management*, 448, 76-84

546 Cao, J., Zhao, B., Gao, L., Li, J., Li, Z., & Zhao, X. (2018). Increasing temperature  
547 sensitivity caused by climate warming, evidence from Northeastern China.  
548 *Dendrochronologia*, 51, 101-111

549 Chen, Z., Yu, G., Ge, J., Sun, X., Hirano, T., Saigusa, N., Wang, Q., Zhu, X., Zhang, Y.,  
550 & Zhang, J. (2013). Temperature and precipitation control of the spatial variation of  
551 terrestrial ecosystem carbon exchange in the Asian region. *Agricultural and Forest  
552 Meteorology*, 182, 266-276

553 Craine, J.M., & Dybzinski, R. (2013). Mechanisms of plant competition for nutrients,  
554 water and light. *Functional Ecology*, 27, 833-840

555 Daly, C., Gibson, W.P., Taylor, G.H., Johnson, G.L., & Pasteris, P. (2002). A  
556 knowledge-based approach to the statistical mapping of climate. *Climate research*, 22,  
557 99-113

558 Davidson, E.A., & Janssens, I.A. (2006). Temperature sensitivity of soil carbon  
559 decomposition and feedbacks to climate change. *Nature*, 440, 165-173

560 Fischer, R., Bohn, F., de Paula, M.D., Dislich, C., Groeneveld, J., Gutiérrez, A.G.,  
561 Kazmierczak, M., Knapp, N., Lehmann, S., & Paulick, S. (2016). Lessons learned from  
562 applying a forest gap model to understand ecosystem and carbon dynamics of complex  
563 tropical forests. *Ecological Modelling*, 326, 124-133

564 Ford, K.R., Breckheimer, I.K., Franklin, J.F., Freund, J.A., Kroiss, S.J., Larson, A.J.,  
565 Theobald, E.J., & HilleRisLambers, J. (2017). Competition alters tree growth responses  
566 to climate at individual and stand scales. *Canadian Journal of Forest Research*, 47, 53-  
567 62

568 Groeneveld, J., Alves, L., Bernacci, L.C., Catharino, E.L.M., Knogge, C., Metzger, J.,  
569 Pütz, S., & Huth, A. (2009). The impact of fragmentation and density regulation on  
570 forest succession in the Atlantic rain forest. *Ecological Modelling*, 220, 2450-2459

571 Guan, D.-X., Wu, J.-B., Zhao, X.-S., Han, S.-J., Yu, G.-R., Sun, X.-M., & Jin, C.-J.  
572 (2006). CO<sub>2</sub> fluxes over an old, temperate mixed forest in northeastern China.  
573 *Agricultural and Forest Meteorology*, 137, 138-149

574 Gundersen, P., Thybring, E.E., Nord-Larsen, T., Vesterdal, L., Nadelhoffer, K.J., &  
575 Johannsen, V.K. (2021). Old-growth forest carbon sinks overestimated. *Nature*, 591,  
576 E21-E23

577 Hao, Z., Li, B., Zhang, J., Wang, X., Ye, J., & Yao, X. (2008). Broad-leaved Korean  
578 pine (*Pinus Koraiensis*) mixed forest plot in Changbaishan (CBS) of China: community  
579 composition and structure. *Journal of Plant Ecology (Chinese Version)*, 32, 238-250

580 He, H.S., Hao, Z., Mladenoff, D.J., Shao, G., Hu, Y., & Chang, Y. (2005). Simulating  
581 forest ecosystem response to climate warming incorporating spatial effects in north-  
582 eastern China. *Journal of Biogeography*, 32, 2043-2056

583 Huang, C., Liang, Y., He, H.S., Wu, M.M., Liu, B., & Ma, T. (2021). Sensitivity of  
584 aboveground biomass and species composition to climate change in boreal forests of  
585 Northeastern China. *Ecological Modelling*, 445, 109472

586 IPCC (2013). *Climate Change 2013: the Physical Science Basis: Working Group I  
587 contribution to the Fifth Assessment Report of the Intergovernmental Panel on Climate  
588 Change*. Cambridge, UK: Cambridge University Press

589 Jiang, Y.-L., Zhou, G.-S., Zhao, M., Wang, X., & Cao, M.-C. (2005). Soil respiration in  
590 broad-leaved and Korean Pine forest ecosystems, Changbai Mountain, China. *Chinese  
591 Journal of Plant Ecology*, 29, 411

592 Keenan, T.F., Gray, J., Friedl, M.A., Toomey, M., Bohrer, G., Hollinger, D.Y., Munger,  
593 J.W., O'Keefe, J., Schmid, H.P., & Wing, I.S. (2014). Net carbon uptake has increased  
594 through warming-induced changes in temperate forest phenology. *Nature Climate  
595 Change*, 4, 598-604

596 Kim, D., Millington, A.C., & Lafon, C.W. (2020). Disturbance after disturbance:  
597 combined effects of two successive hurricanes on forest community structure. *Annals  
598 of the American Association of Geographers*, 110, 571-585



599 Krestov, P., Omelko, A.M., Ukhvatkina, O., & Nakamura, Y. (2015). Temperate  
600 summergreen forests of East Asia. *Ber Reinhold-Tüxen-Ges*, 27, 133-145

601 Lee, H., Jeon, J., Kang, M., Cho, S., Park, J., Lee, M., Lee, H., Kim, D., & Kim, H.S.  
602 (2021). The resilience of the carbon cycles of temperate coniferous and broadleaved  
603 forests to drought. *Forest Ecology and Management*, 491, 119178

604 Li, G.-Q., Bai, F., & Sang, W.-G. (2011). Different responses of radial growth to climate  
605 warming in *Pinus koraiensis* and *Picea jezoensis* var. *komarovii* at their upper  
606 elevational limits in Changbai Mountain, China. *Chinese Journal of Plant Ecology*, 35,  
607 500

608 Liang, P.-H., Wang, X.-P., Wu, Y.-L., Xu, K., Wu, P., & Guo, X. (2016). Growth  
609 responses of broad-leaf and Korean pine mixed forests at different successional stages  
610 to climate change in the Shengshan Nature Reserve of Heilongjiang Province, China.  
611 *Chinese Journal of Plant Ecology*, 40, 425

612 Lyu, S., Wang, X., Zhang, Y., & Li, Z. (2017). Different responses of Korean pine  
613 (*Pinus koraiensis*) and Mongolia oak (*Quercus mongolica*) growth to recent climate  
614 warming in northeast China. *Dendrochronologia*, 45, 113-122

615 Ma, Z., Peng, C., Zhu, Q., Chen, H., Yu, G., Li, W., Zhou, X., Wang, W., & Zhang, W.  
616 (2012). Regional drought-induced reduction in the biomass carbon sink of Canada's  
617 boreal forests. *Proceedings of the National Academy of Sciences of the United States of*  
618 *America*, 109, 2423-2427

619 Oberbauer, S.F., Tweedie, C.E., Welker, J.M., Fahnestock, J.T., Henry, G.H., Webber,  
620 P.J., Hollister, R.D., Walker, M.D., Kuchy, A., & Elmore, E. (2007). Tundra CO<sub>2</sub> fluxes  
621 in response to experimental warming across latitudinal and moisture gradients.  
622 *Ecological Monographs*, 77, 221-238

623 Oliver, C.D., & Larson, B.C. (1996). *Forest stand dynamics. Update edition*. Wiley  
624 New York

625 Peng, C., Zhou, X., Zhao, S., Wang, X., Zhu, B., Piao, S., & Fang, J. (2009).  
626 Quantifying the response of forest carbon balance to future climate change in  
627 Northeastern China: model validation and prediction. *Global and Planetary Change*,  
628 66, 179-194

629 Piao, S., Fang, J., Ciais, P., Peylin, P., Huang, Y., Sitch, S., & Wang, T. (2009). The  
630 carbon balance of terrestrial ecosystems in China. *Nature*, 458, 1009-1013

631 Qian, D.D., Kuang, X., Wang, X.G., Lin, F., Yuan, Z.Q., Ye, J., & Hao, Z.Q. (2019).  
632 Spatio-temporal dynamics of woody plants seed rains in broad-leaved Korean pine  
633 mixed forest in Changbai Mountains from 2006 to 2017, China. *The Journal of Applied*  
634 *Ecology (Chinese)*, 30, 1487-1493

635 Qiu, Y., Gao, L.-S., Zhang, X., Guo, J., & Ma, Z.-Y. (2014). Effect of climate change  
636 on net primary productivity of Korean pine (*Pinus koraiensis*) at different successional  
637 stages of broad-leaved Korean pine forest. *Chinese Journal of Applied Ecology*, 25,  
638 1870-1878

639 Saigusa, N., Li, S.-G., Kwon, H., Takagi, K., Zhang, L.-M., Ide, R., Ueyama, M.,  
640 Asanuma, J., Choi, Y.-J., & Chun, J.H. (2013). Dataset of CarboEastAsia and  
641 uncertainties in the CO<sub>2</sub> budget evaluation caused by different data processing. *Journal*  
642 *of Forest Research*, 18, 41-48

643 Shao, G., Yan, X., & Bugmann, H.J.G. (2003). Sensitivities of species compositions of  
644 the mixed forest in eastern Eurasian continent to climate change. *Global and Planetary*  
645 *Change*, 37, 307-313

646 Tang, F.-d., Han, S.-j., & Zhang, J.-h. (2009). Carbon dynamics of broad-leaved Korean  
647 pine forest ecosystem in Changbai Mountains and its responses to climate change.  
648 *Chinese Journal of Applied Ecology*, 20, 1285-1292

649 Taylor, A.R., Boulanger, Y., Price, D.T., Cyr, D., McGarrigle, E., Rammer, W., &  
650 Kershaw Jr, J.A. (2017). Rapid 21st century climate change projected to shift  
651 composition and growth of Canada's Acadian Forest Region. *Forest Ecology and*  
652 *Management*, 405, 284-294

653 Thom, D., Rammer, W., Dirnböck, T., Müller, J., Kobler, J., Katzensteiner, K., Helm,  
654 N., & Seidl, R. (2017). The impacts of climate change and disturbance on spatio-  
655 temporal trajectories of biodiversity in a temperate forest landscape. *Journal of Applied*  
656 *Ecology*, 54, 28-38

657 Thurner, M., Beer, C., Santoro, M., Carvalhais, N., Wutzler, T., Schepaschenko, D.,  
658 Shvidenko, A., Kompter, E., Ahrens, B., & Levick, S.R. (2014). Carbon stock and  
659 density of northern boreal and temperate forests. *Global Ecology Biogeography*, 23,  
660 297-310

661 Turner, M.G., Romme, W.H., Gardner, R.H., Oneill, R.V., & Kratz, T.K. (1993). A  
662 revised concept of landscape equilibrium-disturbance and stability on scaled landscapes.  
663 *Landscape Ecology*, 8, 213-227

664 Wang, M., Guan, D., Wang, Y., Hao, Z., & Liu, Y. (2006). Estimate of productivity in  
665 ecosystem of the broad-leaved Korean pine mixed forest in Changbai Mountain.  
666 *Science in China Series D: Earth Sciences*, 49, 74-88

667 Wang, M., Li, Q.-r., Xiao, D.-m., & Dong, B.-l. (2004). Effects of soil temperature and  
668 soil water content on soil respiration in three forest types in Changbai Mountain.  
669 *Journal of Forestry Research*, 15, 113-118

670 Wang, W.J., He, H.S., Thompson, F.R., Fraser, J.S., & Dijk, W.D. (2017). Changes in  
671 forest biomass and tree species distribution under climate change in the northeastern  
672 United States. *Landscape Ecology*, 32, 1399-1413

673 Wang, X., Pederson, N., Chen, Z., Lawton, K., Zhu, C., & Han, S. (2019). Recent rising  
674 temperatures drive younger and southern Korean pine growth decline. *Science of the*  
675 *Total Environment*, 649, 1105-1116

676 Wen, X.-F., Yu, G.-R., Sun, X.-M., Li, Q.-K., Liu, Y.-F., Zhang, L.-M., Ren, C.-Y., Fu,  
677 Y.-L., & Li, Z.-Q.J.A. (2006). Soil moisture effect on the temperature dependence of  
678 ecosystem respiration in a subtropical Pinus plantation of southeastern China.  
679 *Agricultural and Forest Meteorology*, 137, 166-175

680 Xie, X., Wang, T., Yue, X., Li, S., Zhuang, B., & Wang, M. (2020). Effects of  
681 atmospheric aerosols on terrestrial carbon fluxes and CO<sub>2</sub> concentrations in China.  
682 *Atmospheric Research*, 237, 104859

683 Yang, M. (1981). The climatic features of Changbaishan and its vertical climatic zone  
684 on the north slope. *Acta meteorologica sinica*, 57-66

685 Yu, G., Song, X., Wang, Q., Liu, Y., Guan, D., Yan, J., Sun, X., Zhang, L., & Wen, X.  
686 (2008). Water-use efficiency of forest ecosystems in eastern China and its relations to

687 climatic variables. *New Phytologist*, 177, 927-937  
688 Yu, G., Wen, X., Li, Q., Zhang, L., Ren, C., Liu, Y., & Guan, D. (2005). Seasonal  
689 patterns and environmental control of ecosystem respiration in subtropical and  
690 temperate forests in China. *Science in China Series D: Earth Sciences*, 48, 93-105  
691 Zhang, J., Zhou, Y., Zhou, G., & Xiao, C. (2014). Composition and structure of *Pinus*  
692 *koraiensis* mixed forest respond to spatial climatic changes. *PloS one*, 9, e97192  
693 Zhao, J., Ma, J., & Zhu, Y. (2019). Evaluating impacts of climate change on net  
694 ecosystem productivity (NEP) of global different forest types based on an individual  
695 tree-based model FORCCHN and remote sensing. *Global and Planetary Change*, 182,  
696 103010  
697 Zhou, L., Dai, L., Wang, S., Huang, X., Wang, X., Qi, L., Wang, Q., Li, G., Wei, Y., &  
698 Shao, G. (2011). Changes in carbon density for three old-growth forests on Changbai  
699 Mountain, Northeast China: 1981–2010. *Annals of Forest Science*, 68, 953-958  
700 Zhuang, L., Axmacher, J.C., & Sang, W. (2017). Different radial growth responses to  
701 climate warming by two dominant tree species at their upper altitudinal limit on  
702 Changbai Mountain. *Journal of Forestry Research*, 28, 795-804